Journal of the European Ceramic Society **17** (1997) 1083–1092

PII: S0955-2219(96)00216-6
0955-2219/97/$17.00

Preparation and Characterization of 2D SiC/SiC Composites with Composition-Graded C(B) Interphase

S. Jacques,[a] A. Guette,[a] F. Langlais,[a] R. Naslain[a] and S. Goujard[b]

[a]Laboratoire des Composites Thermostructuraux, UMR 47 CNRS-SEP-UB1, Université Bordeaux-I, 3, allée de la Boëtie, 33600 Pessac, France
[b]Société Européenne de Propulsion, BP 37, 33165 Saint Médard-en-Jalles, France

(Received 22 March 1996; revised version received 25 September 1996; accepted 21 October 1996)

Abstract

2D SiC/C(B)/SiC composites were prepared by CVI. The C(B) interphase is made of five successive C(B) layers with increasing boron content from the fibre to the matrix. This composition-graded interphase leads to good mechanical properties similar to those obtained with pure pyrocarbon interphase. However, the lifetime in air under load at high temperature of 2D SiC/C(B)/SiC composites is not improved despite the high percentage of boron in several sublayers of the interphase. By TEM characterization, the boron-rich layers were found to exhibit a nano-porous texture probably due to a bad control of the growth process within the fibrous preforms. This nanoporous texture might be responsible for the poor oxidation resistance of these sublayers and consequently the rather short lifetime of the real 2D composites with respect to those previously reported for 1D SiC/C(B)/SiC model microcomposites. © *1997 Elsevier Science Limited.*

1 Introduction

Turbostratic pyrolytic carbon is a classical interphase material in 2D SiC/SiC composites, owing to its ability to deflect the cracks originating in the matrix and to protect the fibre from damage.[1–3] In a recent study on SiC/SiC microcomposites, the addition of boron in a pyrocarbon interphase (up to 33 at%) has been shown to improve the oxidation resistance of these materials but to decrease their mechanical characteristics. By using a composition-graded C(B) interphase, with a boron content increasing from 0 near the fibre to 33 at% near the matrix, microcomposites were obtained with both good mechanical properties and high oxidation resistance.[4]

The present paper deals with the preparation and characterization of this kind of interphase within actual 2D SiC/SiC composites.

2 Experimental

Stacks of 10 fabrics of 2D woven fibres (Nicalon fibre (ceramic grade), Nippon Carbon, Japan), maintained pressed together with a graphite tooling, were chemical vapour infiltrated (CVI) with a composition-graded C(B) interphase (Fig. 1). The synthesis conditions were similar to those used in the previous study carried out on microcomposites.[4] The boron content of this interphase increased from 0 at% B near the fibre to 33 at% B near the matrix. The gaseous precursor was a $C_3H_8/BCl_3/H_2$ mixture and the graded composition of the deposit resulted from a step variation of the initial gas phase ratio $\alpha = 100 \times \frac{Q(BCl_3)}{Q(C_3H_8) + Q(BCl_3)}$ where Q(i) is the partial flow rate of species i. The infiltration durations were selected in order to obtain layers with constant thicknesses and a total interphase thickness of about 0·4 μm (Table 1). The total pressure and temperature of the CVI process were 1·0 kPa and 950°C respectively. After the interphase deposition, some fibres were extracted from the preform and characterized by Auger electron spectrometry (AES) (PHI 590 SAM from Physical Electronics/Perkin Elmer) in order to evaluate the boron concentration gradient.

Finally, the 2D SiC/SiC composites were obtained by CVI of silicon carbide (SiC being the matrix) from a CH_3SiCl_3 (MTS)/H_2 precursor, according to a process which has been described elsewhere.[5]

Three tensile specimens 8·5 cm in length were machined from these composites and were tensile tested at ambient temperature (loading-unloading cycles were performed in one of the tests). The

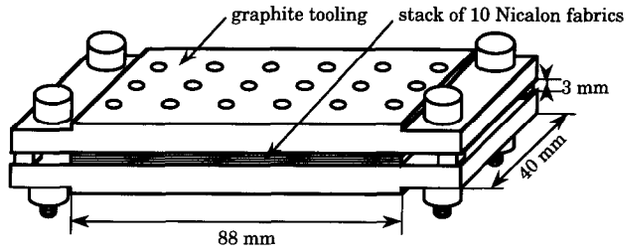

Fig. 1. Graphite tooling in which the stack of Nicalon fabrics is maintained during the CVI process of C(B) interphase (schematic).

Table 1. Infiltration durations and thicknesses of C(B) interphase layers as a function of the initial gas phase[a]

α (%)	Layer	*Infiltration time (min)*	*Mean thickness (nm)*
0	1	240	~80
30	2	8·3	~80
50	3	7	~80
70	4	18	~80
85	5	30	~80

[a]Ratio $\alpha = 100 \times \frac{Q(BCl_3)}{Q(C_3H_8) + Q(BCl_3)}$ where Q(i) stands for the gas flow rate of species i under standard conditions.

tensile stress was calculated from the applied load, assuming that the variations of the specimen cross-section area during loading could be neglected. The tensile strain was measured with an extensometer with a 25 mm gauge length. Six other test samples (0·33 × 1 × 6 cm^3) were submitted to air ageing treatment at high temperature and under a constant load in four point bending corresponding to a stress of 150 MPa. Two samples were tested at 500°C, two at 600°C and two at 700°C.

Three types of sample were characterized by transmission electron microscopy (TEM) (CM 30 ST from Philips, The Netherlands). The first was taken from a sample which had been submitted to the ambient tensile test with load cycles (Fig. 2(a)). The second was taken from a specimen which had been aged under a four point bending load corresponding to a stress of 150 MPa at 600°C (Fig. 2(b)) and the third was made of fibres extracted from a 2D preform infiltrated only with the C(B) composition-graded interphase. Thin foils were prepared for the two first samples according to a classical procedure, i.e. the composite was embedded in an epoxy resin, the interesting parts were cut off with a diamond wire saw, thinned by mechanical polishing and then ion milling (600 Duo Mill from Gatan, USA). For the third sample, a specific procedure already described for the microcomposites study was used.[6] The C(B) interphases were observed in TEM using bright field and high resolution techniques. For symmetrical C-002 lattice imaging, an 11·5 nm^{-1} objective opening was used. The interphase composition was analysed locally by electron energy loss spectroscopy (EELS; Gatan) with a probe diameter of about 20 nm.

3 Results and Discussion

3.1 AES interphase characterization

Figure 3 gives the atomic concentration profiles within the interphase measured by AES in-depth and near the external surface of 2D SiC/C(B)/SiC composites preforms. Carbon and boron contents are similar to those obtained previously in SiC/C(B)/SiC microcomposites.[4] On the other hand, the infiltration leads to different thicknesses of this interphase between the centre and the periphery of the 2D preform (400 nm and 800 nm, respectively, obtained through a sputter rate calibrated with Ta_2O_5 layers).

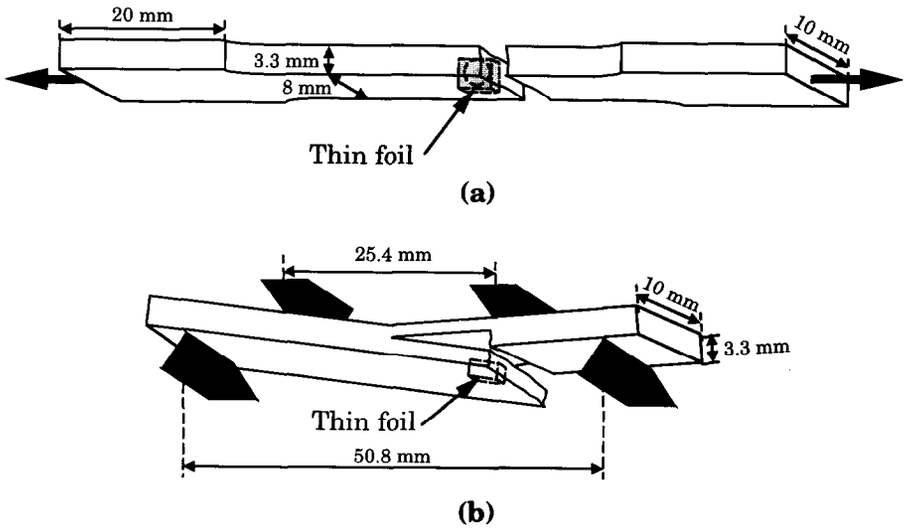

Fig. 2. Location of the thin foil sample after failure in (a) the tensile test specimen and (b) the bending test specimen.

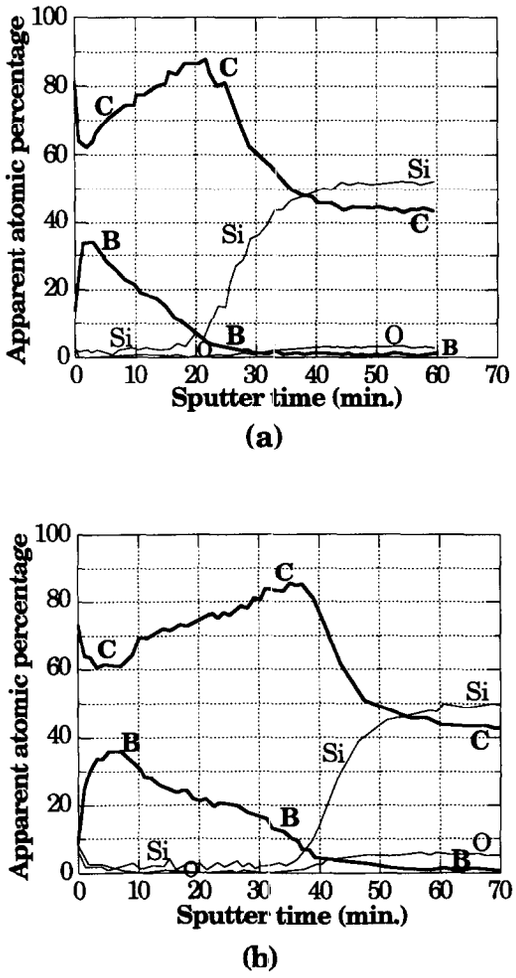

Fig. 3. AES depth atomic concentration profiles for the C(B) composition gradient interphase (a) in the centre and (b) on the periphery of the fibrous preform prior to matrix infiltration. (Sputter rate: 20 nm/min; ref. Ta_2O_5).

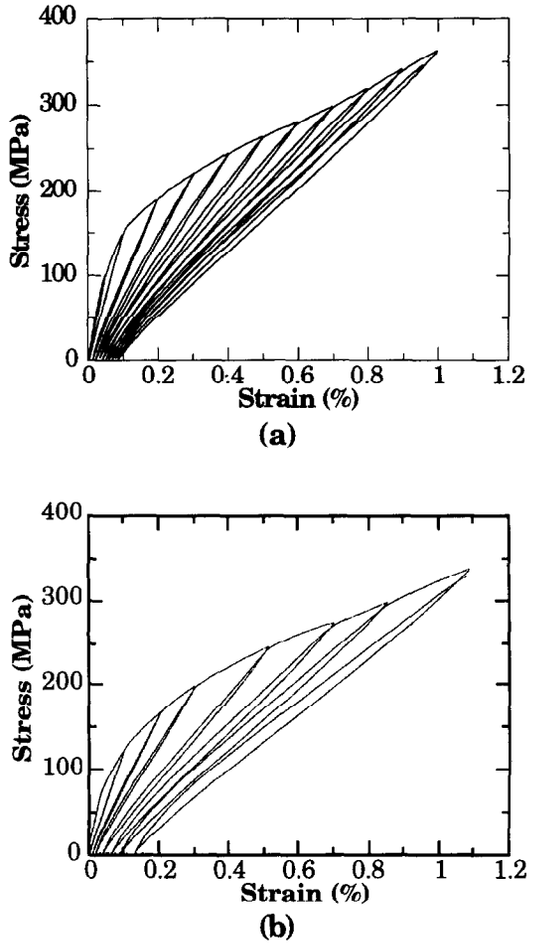

Fig. 4. Tensile stress–strain curves with load cycles for (a) 2D SiC/PyC/SiC and (b) 2D SiC/compositional gradient C(B)/SiC.

3.2 Ambient tensile tests

The strain and stress to failure of the three tensile-tested 2D SiC/C(B)/SiC samples were 0·96% and 330 MPa, 1·1% and 340 MPa and 1·1% and 350 MPa. The proportional limit was about 65 MPa. These values are very close to those obtained for SiC/PyC/SiC composites[7] containing a pyrocarbon interphase, as previously reported for microcomposites.[4] Figure 4 shows the tensile test curves with loading-unloading cycles for both types of 2D composite. The behaviours are very similar. The hysteresis loops exhibit, at the end of the loading cycles, a linear part which intersects the origin of the stress-strain coordinate axes. This is typical behaviour for damageable elastic material. Nevertheless, some difference is apparent between the two types of composite. The curvature of the non-linear domain is lower and more smooth up to 0·2% in strain for the C(B) composition-graded interphase. Moreover, after being submitted to equivalent stresses, the samples with C(B) interphases exhibit residual strains 50% higher and hysteresis loop areas 30% larger than for their counterparts with PyC interphases. This difference suggests that the C(B) graded-composition interphase leads to a slightly weaker fibre-matrix bond than the classical PyC interphase.[8]

3.3 Oxidation resistance

The 2D SiC/C(B)/SiC composites, submitted to ageing treatments in air under bending loading, exhibit lifetimes of 513–601 h at 500°C, 22–43 h at 600°C and 4–7 h at 700°C. These values are of the same order as those obtained under similar conditions for the classical 2D SiC/PyC/SiC composites (pers. comm.) The improvement in lifetime of SiC/C(B)/SiC with respect to SiC/PyC/SiC, previously obtained for microcomposites,[4] could not be found again in the case of 2D composites. Two possible reasons for this difference can be put forward. The first may be related to the difference in the applied load pattern, namely tensile ageing at a stress close to the proportional limit for the microcomposites and bending ageing at a stress much above the proportional limit for the 2D actual composite. The second could be a difference between the microstructure of the C(B) graded-composition interphase in the microcomposite (CVD process)

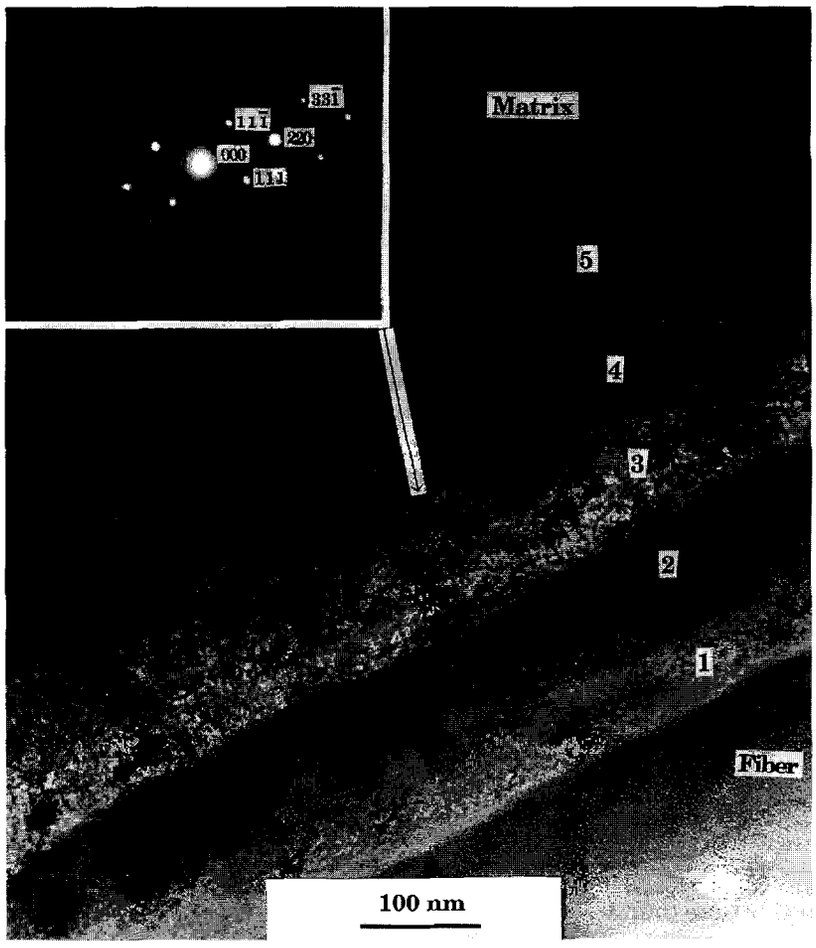

Fig. 5. Bright-field TEM image of the interphase with microdiffraction (inset) of a SiC nanocrystal entrapped in layer 4.

and the 2D composite (CVI process), although the composition gradient is similar in both cases, as shown by the AES profiles.[4]

3.4 TEM characterization of 2D SiC/C(B)/SiC composites

3.4.1 C(B) interphase in the composite

Figure 5 gives a bright field image of the C(B) interphase close to a transverse fibre (here the thin foil was taken from a sample submitted to tensile test). Layers 1 and 2 are clearly apparent owing to a marked difference in contrast. The first appears as a uniformly light grey, probably related to a poorly organized pyrocarbon. In contrast, the second exhibits (i) a columnar microstructure of the C(B) with a growth direction perpendicular to the fibre surface and (ii) a high level of crystallization indicated by a dark grey contrast. The layers 3 and 4 are very similar with a high contrast, including dark zones (probably nano-sized well-crystallized grains) embedded in bright zones, corresponding to amorphous parts and/or nanoscale pores. Layer 5 is difficult to distinguish from the matrix, a feature which could result from a partial infiltration of SiC within this part of the interphase.

Figure 6 shows the EELS spectrum for each layer of the C(B) graded interphase. Carbon (K edge at 284 eV) and boron (K edge at 188 eV) are detectable and the boron content increases from layer 1 to layer 4. In layer 5, a silicon peak ($L_{2,3}$

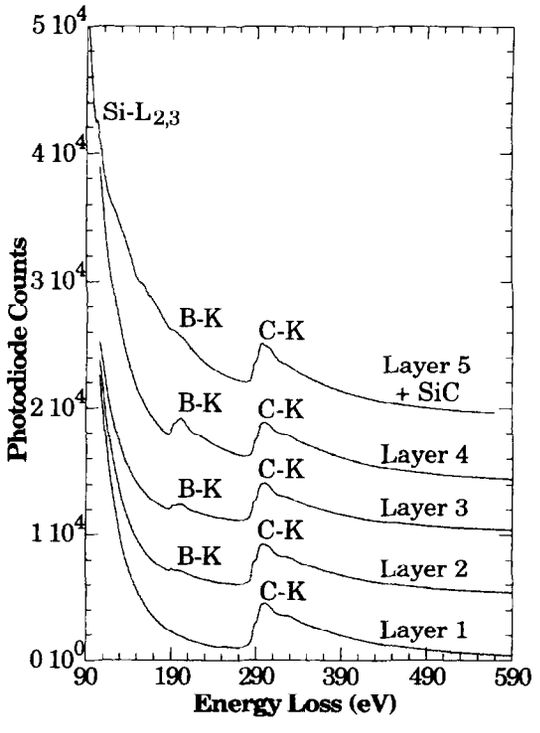

Fig. 6. EELS spectrum from the CVI C(B) interphase with a composition gradient.

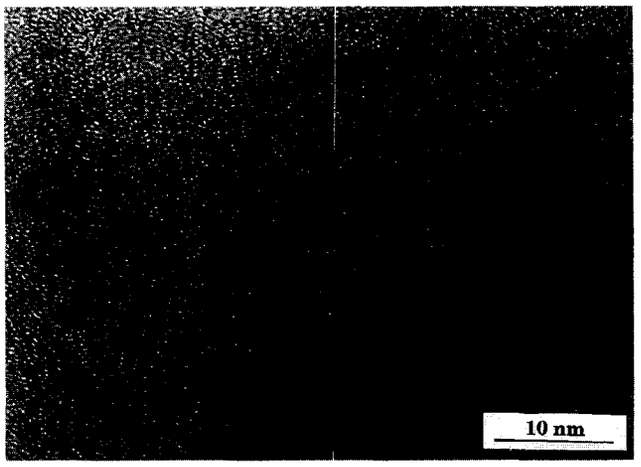

Fig. 7. HRTEM image of layer 1.

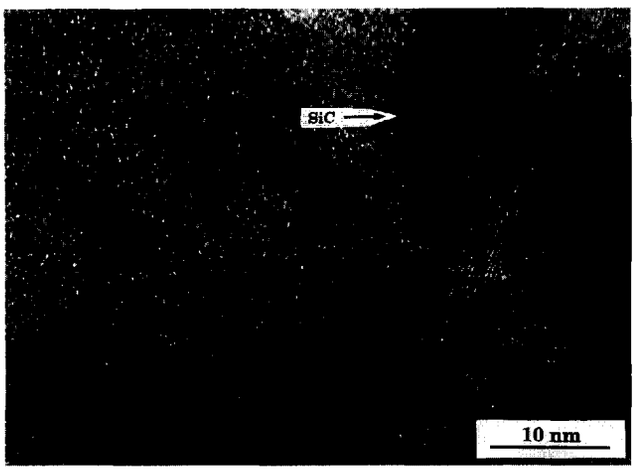

Fig. 9. HRTEM image of layer 4.

edge at 99 eV) is observed, which partially overlaps the boron peak. This last result seems to confirm the occurrence of some infiltration of SiC within the matrix side part of the interphase.

The very dark nanometric crystals (up to 20 nm in size) visible in the bright field image of layers 3 and 4 were analysed by microdiffraction (with a spot size of 10 nm), as shown in Fig. 5. The pattern obtained is, quite surprisingly, that of β-SiC nanocrystals.

On the basis of all these observations for layers 3 to 5, a nano-porous C(B) microtexture can be suggested, whose porosity is partially filled with SiC nanocrystals.

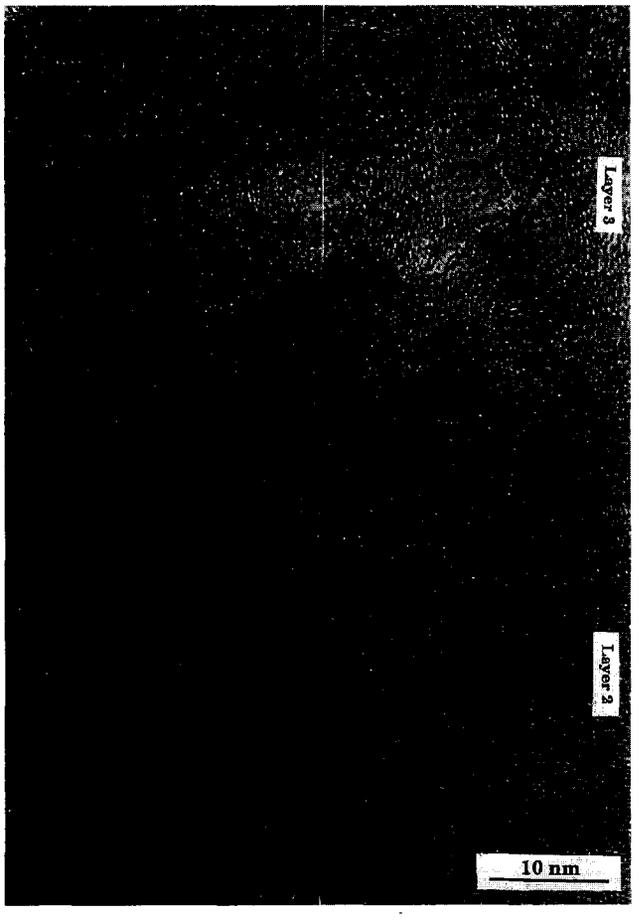

Fig. 8. HRTEM image of layers 2 and 3.

Further investigations on the various parts of this C(B) composition graded interphase were carried out by high resolution transmission electron microscopy (HRTEM). The image of layer 1 can be related to a weakly organized pyrocarbon, with only a slight anisotropy (Fig. 7). This type of pyrocarbon is very similar to the one obtained under identical conditions by CVD for microcomposites.[4] Layer 2, shown in the lower part of the image in Fig. 8, exhibits a very high anisotropy with the carbon layer stack oriented parallel to the fibre axis. This layer is also very similar to the corresponding layer obtained by CVD in microcomposites.[4] Layers 3 (upper part of Fig. 8) and 4 (Fig. 9) reveal lattice fringes with marked contrasts and carbon layer stacks which form winding sheets (about 5 nm in width and up to 50 nm in length) without preferred orientation. At the interface between layers 2 and 3, stacks of layer 3 occur perpendicular to stacks of layer 2. Between these sheets, weakly contrasted zones (about 10 nm in size) appear which could be (i) amorphous solid, (ii) crystals whose orientation does not fulfil the Bragg conditions or (iii) porosity. In the HRTEM image of layer 4 (Fig. 9), nanocrystals of β-SiC (with (111) planes slightly visible) were evidenced as in the bright field images (Fig. 5). The occurrence of such nanocrystals seems to confirm the presence of nanoporosity within layers 3 and 4. This sponge-like nanotexture is very different from the more dense nanotexture of corresponding interphase layers resulting from CVD in the microcomposites.[4]

3.4.2 C(B) interphase prior to matrix infiltration

In order to understand the effect of matrix infiltration on the nanostructure of the C(B) graded interphase in the 2D composites, the interphase was observed before infiltration using TEM. A

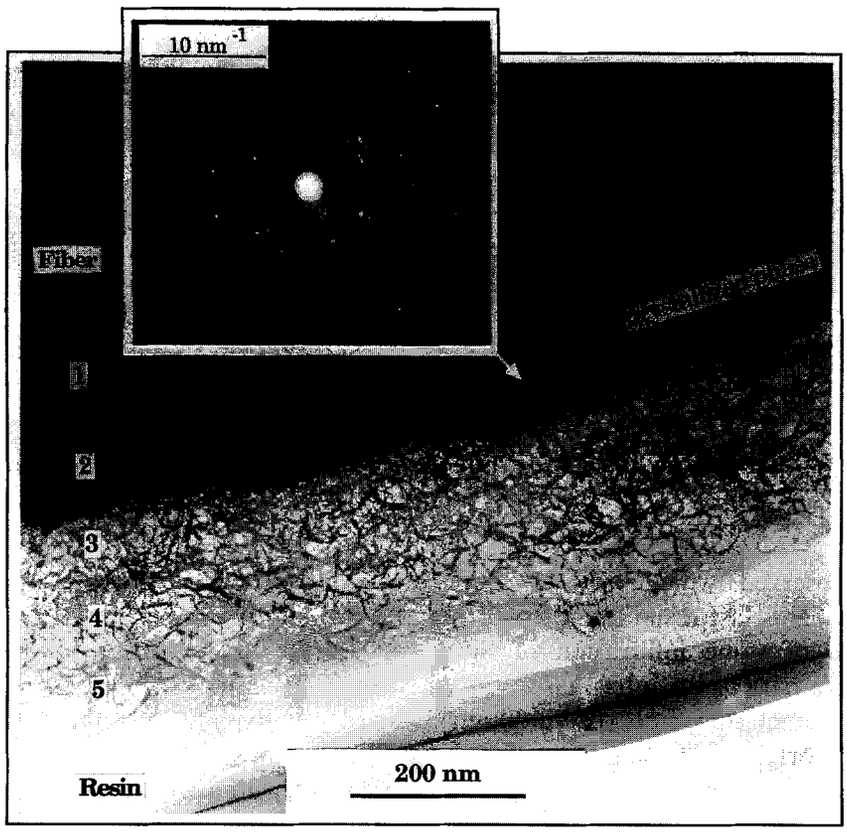

Fig. 10. Bright-field TEM image of the interphase prior to matrix infiltration with an electron SAD pattern (inset) from the particulate phase present in layer 2 prior to matrix infiltration.

high magnification bright field image (Fig. 10) also shows a nanoporous microtexture for layers 3, 4 and 5, but these layers cannot be distinguished.

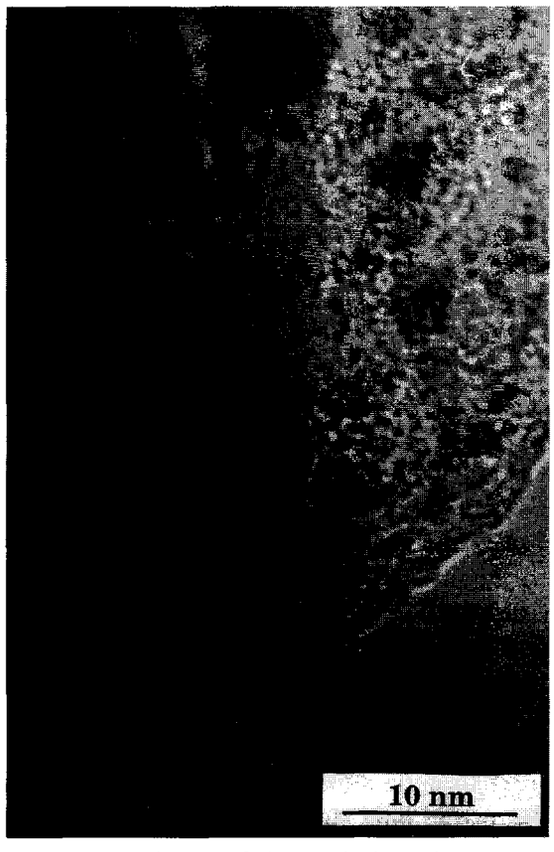

Fig. 11. HRTEM image of the particulate phase present in layer 2 prior to matrix infiltration.

On the other hand, layer 2 contains isolated crystals similar to those observed in the corresponding layer of the C(B) interphase in microcomposites. Identical reticular distances are deduced from a selected area diffraction pattern recorded for these crystals (Fig. 10). (111) lattice fringes of this phase are visible in Fig. 11. This HRTEM observation shows that these crystals are mixed here with amorphous carbon due to an Ar^+ ion milling effect.

Thus, the infiltration of the matrix in the 2D composites is not the cause of the sponge-like nanotexture of the boron-rich part of the C(B) graded interphase, the corresponding layers being slightly infiltrated by SiC. Conversely, the isolated crystals, identified as a diamond-like structure with many stacking faults in microcomposites,[4] seem to have disappeared during the densification (i.e. at 1000°C and during several hundred hours), which is consistent with the metastable nature of the nanocrystals.

The nanoporous texture observed for layers 3, 4 and 5 could result from the stagnation of by-products (such as HCl) together with the reactive species within the fibrous preform. The growth rate of such boron-rich layers being very high,[9] HCl and H_2 species could be trapped inside the solid deposit which could lead to the formation of partly open nanopores. Consequently, the SiC matrix could be infiltrated within such layers.

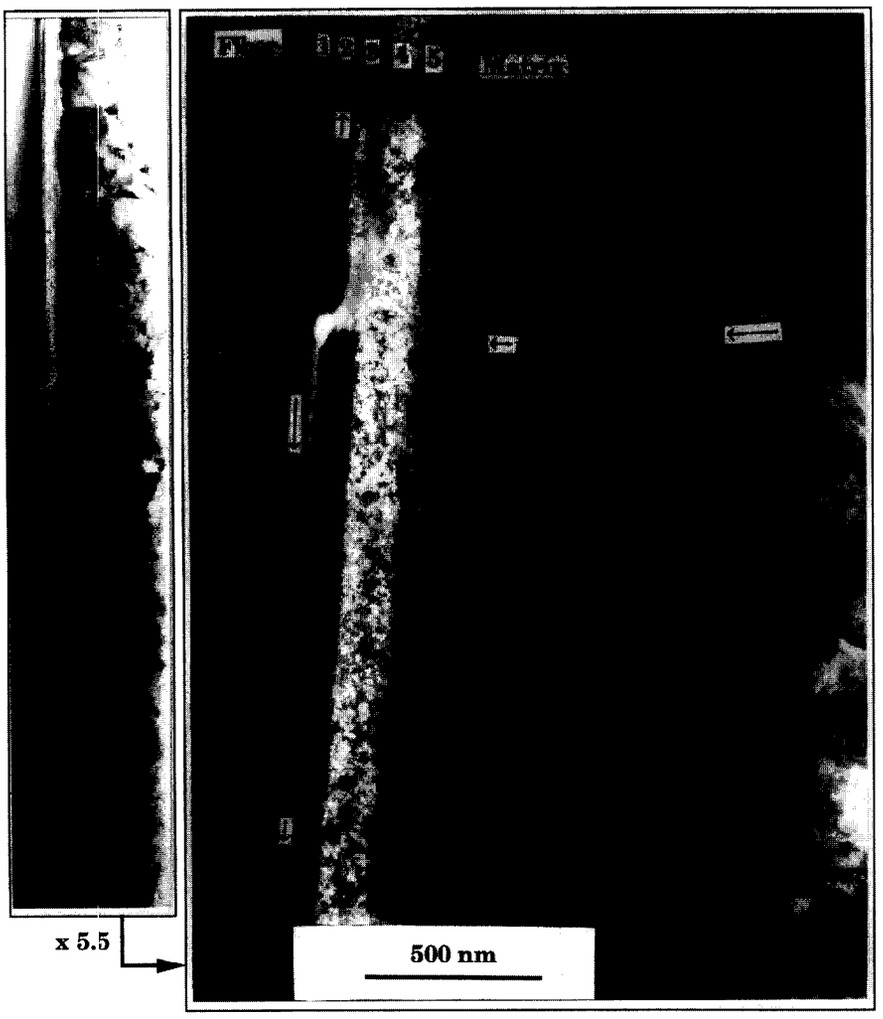

Fig. 12. Bright-field TEM images showing matrix crack deflection in the composition gradient interphase.

3.4.3 Localization of deflected matrix cracks

As shown in Fig. 12, the tensile test resulted in deflection of the matrix cracks and their propagation mostly within layer 2, i.e. the most organized layer. The nanoporous part of the interphase (layers 3 to 5) does not deflect the crack. Layer 2 seems to be responsible for the good ambient mechanical properties of the composite. This feature is consistent with the assumption that matrix crack deflection is favoured in an interphase displaying a layered crystal structure or a layered microstructure.[10] Figure 13 shows another crack deflection which occurs between layers 2 and 3 as in microcomposites.[6]

3.4.4 C(B) interphase after ageing test

To try to explain the relatively weaker behaviour of the present 2D SiC/C(B)/SiC composites when submitted to an ageing treatment in air under load, the C(B) graded-composition interphase was observed by TEM after such a test.

TEM bright field observations have shown that only the interphases deposited on transverse fibres (i.e. perpendicular to the sample axis) have been oxidized. This result can be explained by (i) the shorter route for oxygen diffusion along these fibres than along the longitudinal fibres and (ii) the localization of the matrix cracks in the plane of transverse fibres, the corresponding interphases being more rapidly exposed to air.

The bright field image in Fig. 14 shows a zone of the interphase where it has been partially oxidized. Layers 1, 3, 4 and 5 were replaced by an amorphous material (its electron diffraction pattern is a diffuse halo) which seems to contain bubbles possibly entrapped in the sample during cooling. EELS analysis shows that this material consists mainly of silica, as for the oxidized interphase in microcomposites. Layer 2 in the present 2D composite seems to have better resistance to oxidation for it was only partially replaced by silica, as shown in the EELS spectrum of Fig. 14. The more rapid consumption of layer 1 can be attributed to the absence of boron, whereas that of layers 3, 4 and 5 can be assigned to their porous nanotexture which gives them a high specific surface exposed to air. Finally, Fig. 15 shows another region of the oxidized interphase where all the layers are replaced by silica, as confirmed by EELS analysis.

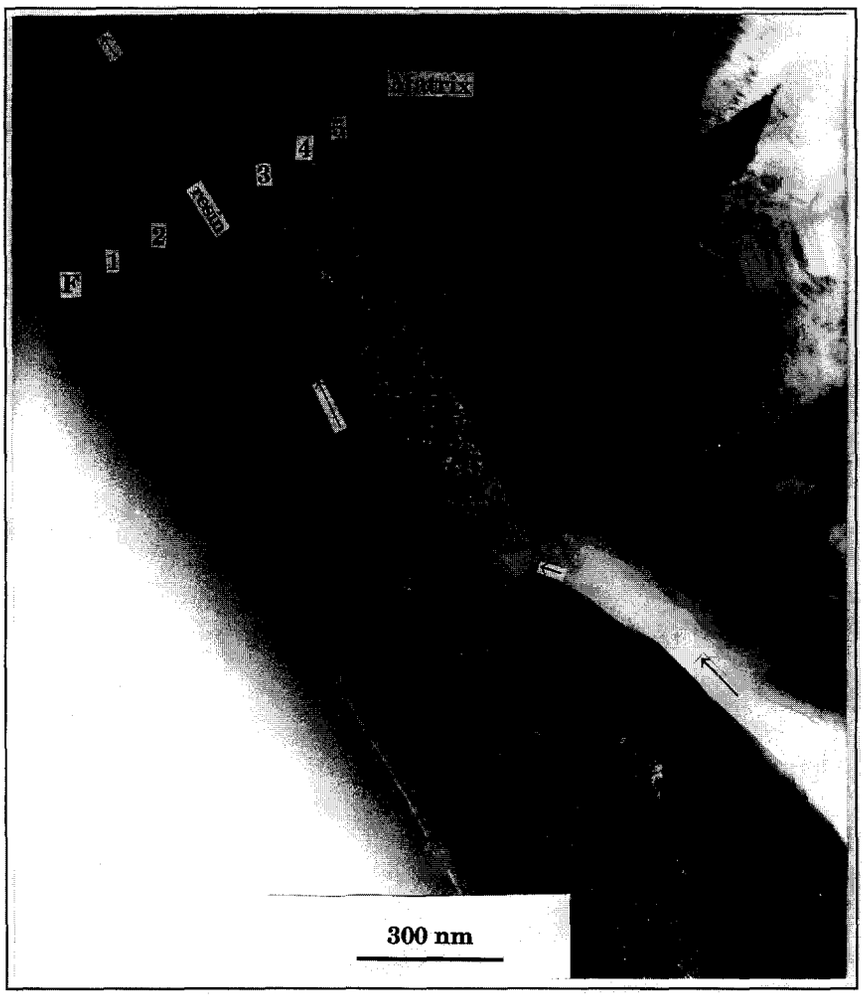

Fig. 13. Bright-field TEM image showing matrix crack deflection in the composition gradient interphase.

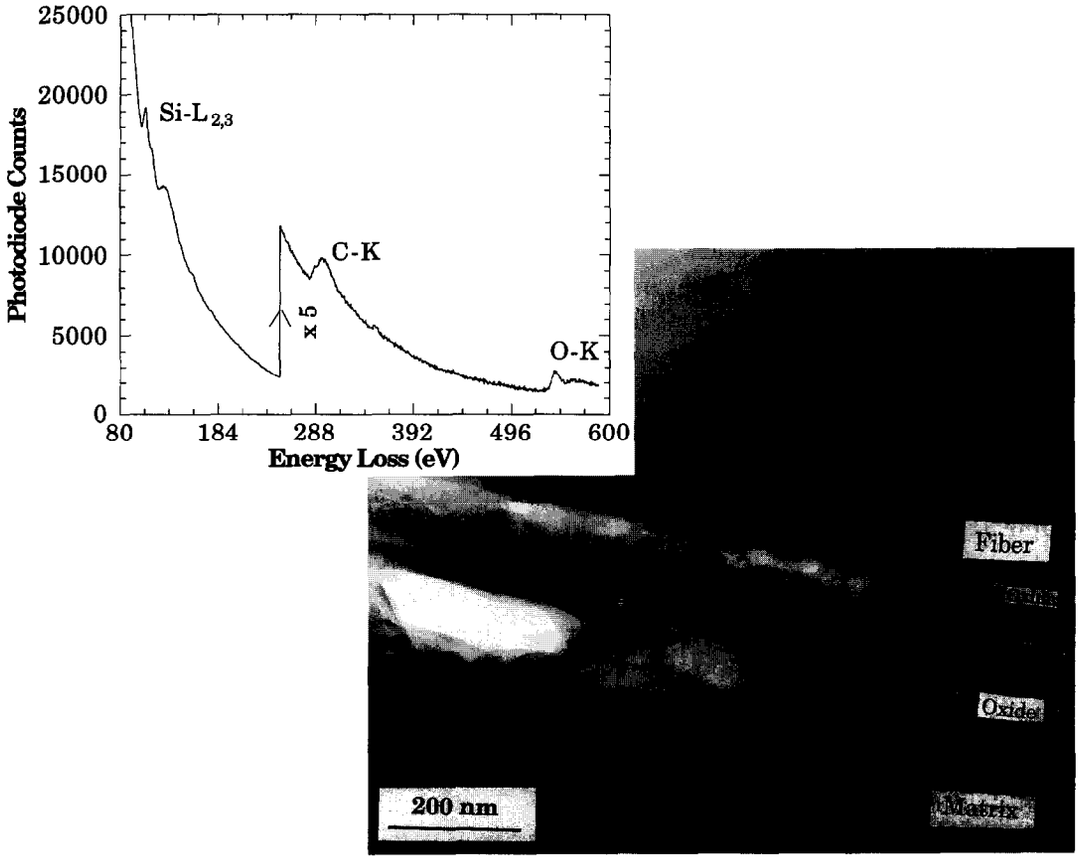

Fig. 14. Bright-field TEM image of the partially oxidized composition gradient interphase (inset: EELS spectrum from the partially oxidized layer 2).

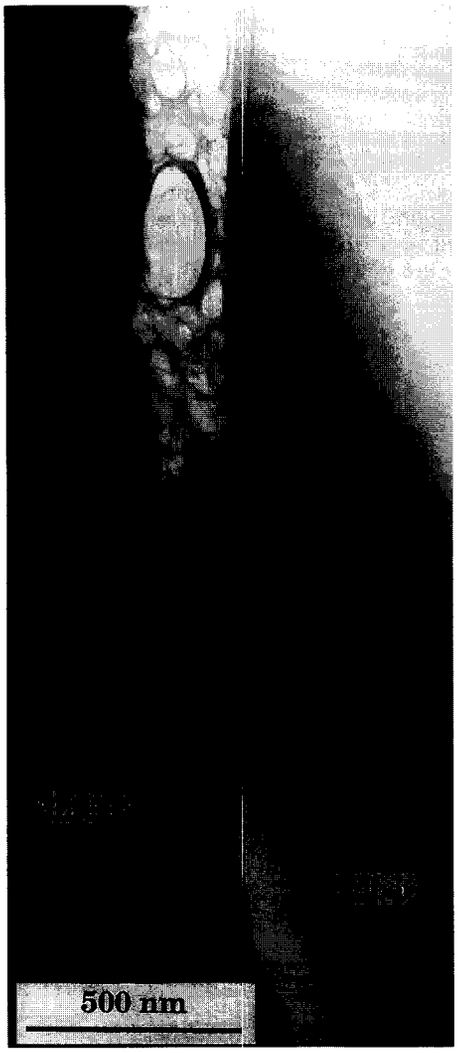

Fig. 15. Bright-field TEM image of the oxidized composition gradient interphase.

In the various samples observed by TEM after ageing, the absence of boron in the oxidized interphases could be explained by the extreme reactivity of boron oxide towards water vapour in air, giving rise to boric acid which is highly volatile even at ambient temperature.[11] This phenomenon could be enhanced during the thin foil preparation.

4 Conclusion

2D SiC/SiC composites with a composition-graded C(B) interphase made of five layers (with a boron content increasing from the fibre to the matrix) were prepared by CVI. This interphase results in ambient mechanical characteristics of the 2D composites similar to those of the corresponding material with a pure pyrocarbon interphase. On the other hand, it seems not to favour an increase in the lifetime of such composites when submitted to thermal ageing in air under load, in contrast to a similar interphase reported[4] to increase the lifetime of their microcomposite counterparts.

These effects have been explained through TEM characterization of the interphase before and after matrix infiltration as well as after thermal ageing. The two first layers close to the fibre (pure pyrocarbon and 8 at% boron C(B) material) are very similar to those obtained by CVD in microcomposites. Layer 2 is a highly organized turbostratic boron-doped carbon. The diamond-like nanocrystals observed in microcomposites[4] seem to have disappeared during the CVI of the SiC matrix. In contrast, the layers close to the matrix (layers 3, 4 and 5) exhibit a texture highly different from those in the microcomposites; they have a sponge-like character with numerous nano-pores. This texture, in conjunction with the drastic damaging test (high level bending load), could explain the low lifetime observed for these composites, owing to a rapid diffusion of oxygen within (i) the numerous cracks of the matrix and (ii) the internal porosity of such layers.

A better control of the growth process of the boron-rich layers in the interphase infiltration in order to obtain dense films could improve the lifetime of the real composites and lead to a behaviour similar to that previously reported for the microcomposites.

Acknowledgements

This work has been supported by CNRS and SEP through a grant to S.J. The authors wish to thank SEP for mechanical and ageing tests and are grateful to F. Doux from SEP, X. Bourrat and H. Tenailleau from LCTS, and M. Lahaye from CUMENSE for fruitful discussion.

References

1. Naslain, R., Fiber-matrix interphases and interfaces in ceramic-matrix composites processed by CVI. *Composite Interfaces*, 1993, **1**, 253–286.
2. Evans, A. G. and Zok, F. W., The physics and mechanics of fibre-reinforced brittle matrix composites. *J. Mater. Sci.*, 1994, **29**, 3857–3896.
3. Jouin, J. M., Cotteret, J. and Christin, F., SiC/SiC interphase: case history. In *Proc. 2nd European Colloquium Designing Ceramic Interfaces*, CEE Joint Research Centre, Petten, NL, 11–13 Nov 1991.
4. Jacques, S., Guette, A., Langlais, F. and Naslain, R., C(B) materials as interphases in SiC/SiC model microcomposites. *J. Mater. Sci.*, submitted.
5. Naslain, R., Rossignol, J. Y., Hagenmuller, P., Christin, F., Heraud, L. and Choury, J. J., Synthesis and properties of new composite materials for high temperature applications based on carbon fibers and C–SiC or C–TiC hybrid matrices. *Rev. de Chim. Min.*, 1981, **18**, 544–564.
6. Jacques, S., Guette, A., Langlais, F. and Bourrat, X., Characterization of SiC/C(B)/SiC microcomposites by transmission electron microscopy. *J. Mater. Sci.*, submitted.

7. Guillaumat, L., Microfissuration des CMC: relation avec la microstructure et le comportement mécanique. PhD thesis No 1056, University of Bordeaux I, France, 1994.
8. Droillard, C., Lamon, J. and Bourrat, X., Strong interface in CMCs, condition for efficient multilayered interphases. In *Mat. Res. Soc. Symp. Proc.*, Nov. 1994, ed. R. A. Lowden, J. R. Hellmann, M. K. Ferber, S. G. Di Pietro and K. K. Chawla. Materials Research Society, 1995, Vol. 365, 371–376.
9. Jacques, S., Guette, A., Bourrat, X., Langlais, F., Naslain, R., Guimon, C. and Labrugère, C., LPCVD and characterization of boron-containing pyrocarbon materials. *Carbon*, 1996, **34**(9), 1135–1143.
10. Naslain, R., The concept of layered interphases in SiC/SiC. In *Ceram. Trans.*, ed. A. G. Evans and R. Naslain. The Amer. Ceram. Soc., Westerville, OH, USA, 1995, vol. 58, 23–39.
11. Kobayashi, K., Maeda, K., Sano, H. and Uchiyama, Y., Formation and oxidation resistance of the coating formed on carbon material composed of B_4C-SiC powders. *Carbon*, 1995, **33**, 397–403.